High Mass Flux Tests on Catalytic Beds for H$_2$O$_2$ Monopropellant Thruster

Angelo Pasini [1], Lucio Torre [2], Luca Romeo [3], Angelo Cervone[4], Luca Masi[5] and Luca d'Agostino[6]

ALTA S.p.A. - 5 Via A. Gherardesca - 56121 Ospedaletto, Pisa, Italy

The present paper illustrates the results of an experimental campaign carried out using LR-III-106 catalyst developed by ALTA S.p.A. in collaboration with the Chemical Department of Pisa University. The catalytic bed has been integrated into a hydrogen peroxide monopropellant thruster prototype and tested in ALTA's Green Propellant Rocket Test Facility. Endurance tests on LR-III-106 catalyst had been already performed with the same thruster prototype at a lower mass flux ($G \approx 12$ kg/(m^{2}s)): the bed was able to decompose up to 13 kg of 90% hydrogen peroxide, equivalent to 2500 s of thruster continuous operation, exhibiting C-Star efficiency higher than 95%. The tests reported in the present paper have been aimed at investigating the performance of the catalyst and the thruster with a mass flux increased up to 55 kg/(m^{2}s). The bed has shown high decomposition and propulsive efficiencies, well in excess of 90%. The cold start-up transient has been reduced to about 1 s, one order of magnitude lower than the previous obtained at lower G.

Nomenclature

A	=	cross sectional area ($A = \pi D^2/4$)
A_t	=	throat area ($A_t = \pi D_t^2/4$)
C_h	=	Stanton number
c^*	=	characteristic velocity
$c_{p\,bed}$	=	constant pressure specific heat of the bed
$c_{p\,flow}$	=	constant pressure specific heat of the reacting flow
D	=	catalytic bed diameter
D_t	=	throat diameter
F	=	thrust
G	=	bed load or mass flux ($G = m/A$)
I_{sp}	=	specific impulse
L	=	catalytic bed length
m	=	propellant mass flow rate
p_c	=	chamber pressure
R	=	gas constant of the exhaust gases
$\dot{r}$	=	volumetric molar reaction rate
S_{bed}/m_{bed}	=	surface area per unit mass of the catalyst

[1] Ph.D. Student, Aerospace Engineering Department, Pisa University - Project Engineer, ALTA S.p.A., AIAA Member; a.pasini@alta-space.com

[2] Project Manager, ALTA S.p.A., AIAA Member; l.torre@alta-space.com

[3] Ph.D. Student, Aerospace Engineering Department, Pisa University - Project Engineer, ALTA S.p.A., AIAA Member; l.romeo@alta-space.com

[4] Project Manager, ALTA S.p.A., AIAA Member; a.cervone@alta-space.com

[5] M.S., Aerospace Engineering Department, Pisa University; lucamasi83@libero.it

[6] Professor, Aerospace Engineering Department, Pisa University, AIAA Member; luca.dagostino@ing.unipi.it

T_{ad}	=	adiabatic decomposition temperature
T_{amb}	=	ambient temperature
$\bar{T}_{bed}$	=	mean temperature of the bed
T_c	=	combustion chamber temperature
$T_{1,...,5}$	=	temperatures at different stations along the bed
V_{bed}	=	volume of the bed
γ	=	specific heat ratio of the exhaust gases
η_{c^*}	=	characteristic velocity efficiency
$\eta_{\Delta T}$	=	temperature efficiency
ε_{bed}	=	macroscopic porosity of the bed
τ	=	residence time
$\Delta \bar{T}$	=	difference between the mean temperature of the bed and the mean temperature of the reacting flow

I. Introduction

SINCE the Black Arrow flight in 1971 hydrogen peroxide has seldom found application as propellant in flight propulsive subsystems. This trend has partially changed in the last years, when several research teams all over the world have started to direct their efforts toward the optimization of the critical components of a propulsion subsystem operating with hydrogen peroxide. In this context, the catalytic bed is probably the most important among the elements to be further developed.

In the last four years Alta S.p.A., in collaboration with the Departments of Chemistry of Pisa and Messina Universities, has studied different combinations of preparation techniques and substrates in order to develop a durable catalytic bed for H_2O_2 decomposition[1,2,3]. The most effective catalyst configurations have been jointly tested on different monopropellant thruster prototypes to evaluate the propulsive parameters such as specific impulse, efficiencies and duration[4]. One of the main goals has been achieved with the catalytic beds LR-III-106 and CZ-11-600 which have been respectively capable to decompose up to 13 and 11 kg of 90% hydrogen peroxide, equivalent to 2500 s and 2000 s of thruster continuous operation[5]. Nevertheless these catalyst lifetimes have been obtained with a bed load of 12 kg/(m²s) which is far from the lower limit of mass flow reported in literature for HTP monopropellant thruster. Typical bed loads for H_2O_2 catalysts are reported[6] to range from a lower limit of 35 kg/(m²s) to a maximum of 279 kg/(m²s) even though General Kinetics Inc. claimed[7] to have successfully tested a catalytic bed with a mass flux of 976 kg/(m²s) but no information about the catalyst used in this specific case are provided.

In the field of miniature HP thrusters, Scharlemann et al.[8] have developed a prototype operating with a monolithic catalyst able to significantly reduce the pressure drop across the catalytic bed compared to pellet configurations. The advanced catalyst has been able to decompose up to 1.2 kg of H_2O_2 for a total catalyst lifetime of 1.25 hrs and a total impulse of 1600 Ns. Being the generated thrust level between 50 to 550 mN, the bed load has been limited to about 2 kg/(m²s). Another interesting work, carried out by KAIST (Korean Advanced Institute of Science and Technology)[9], was concerned with the sizing of a 50 N thruster using the results of experiments performed on a catalytic reactor at low mass flow. For both devices a bed load of 50 kg/(m²s) has been used. The catalyst was similar to those recently developed by Alta S.p.A. and consisted of a bimodal γ–Al_2O_3 pellet substrate impregnated with platinum using H_2PtCl_6 solution as a precursor. For this reason it has been decided to choose a similar bed load for the experiments presented in the present work. By replacing the nozzle with a new one of larger throat diameter than that used with a bed load of 12 kg/(m²s), Alta's monopropellant thruster prototype[5] has been adapted to operate with an increased G factor of 55 kg/(m²s). The thruster has been fired for about 100 seconds, partly in continuous and partly in pulsed mode, using the LR-III-106 catalytic bed. The generated thrust has been about 32 N and the efficiencies have been higher than 90%.

II. Experimental Apparatus

A. Thruster Prototype, Test Facility and Instrumentation

The monopropellant thruster prototype is the same used in the previous test campaign (Pasini et al.[5]). Its design allows for easily changing the principal operational parameters as the chamber pressure p_c, by mounting different nozzles which have been manufactured as separate elements and the hydrogen peroxide dwell time into the bed, τ,

by the possibility of setting both the mass flux G (by means of interchangeable cavitating venturis placed along the hydrogen peroxide feeding line) and the bed length L.

The thruster (see Figure 1) consists of four main parts which are:

- the AISI 316L cylindrical casing (part 5) which is interfaced at the fore end with the flanged connection to the thrust balance (part 8) and at the aft end to the threaded nozzle (part 9);
- the AISI 316L exhaust nozzle (part 9), which is screwed in the aft part of the casing;
- the hydrogen peroxide injection system which is realized by means of a hollow-cone fine spray nozzle (part 2), assembled on the adapter (part 3) by means of a ring nut (part 4). For the present experimental campaign the model TN-SS-18 by Spraying System Co. has been used: it nominally operates at 25.5 g/s of water with 5 bar of pressure drop generating droplets with 110 μm volumetric mean diameter and a jet angle of 58°.
- The catalytic bed which is retained between an AISI304 cap-shaped grid (part 6) with a 40 mesh index injection plate loaded by means of a 20 N stainless steel compression spring (part 11) and the distribution plate (part 7), with 50% open area ratio, realized by means of 210 x 1.5 mm I.D. holes for more uniform injection the decomposition products in the combustion chamber. The maximum volume available for the catalytic bed in the channel between the injection and distribution plates is 30 cm^3, with a maximum length of 60 mm.
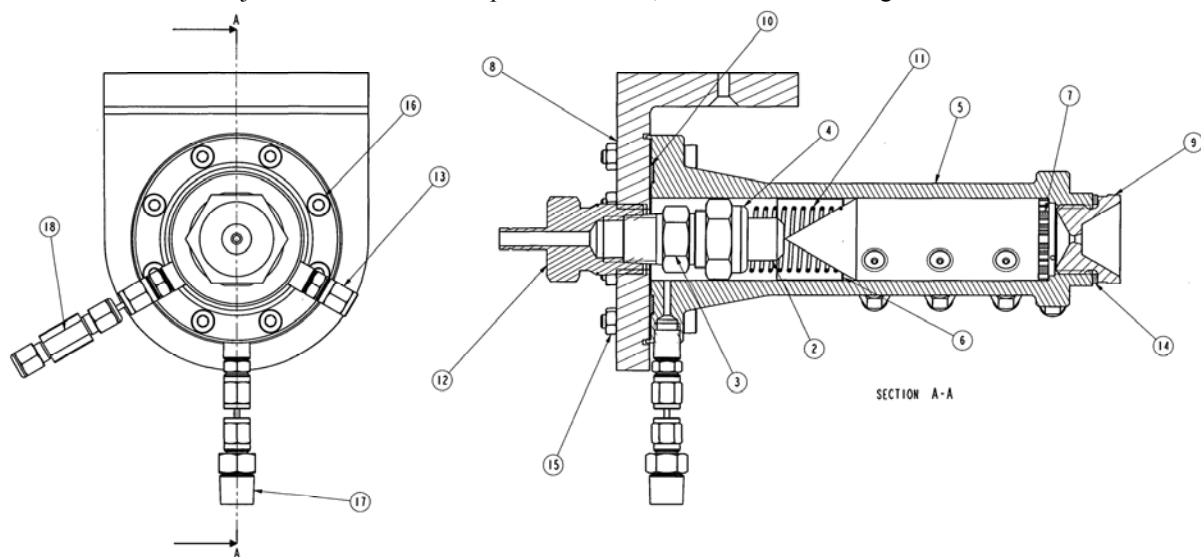

Figure 1. Drawing of the hydrogen peroxide monopropellant thruster prototype.

The sealing between the L-shaped connection (part 8) with the thrust balance of Alta's Green Propellant Rocket Tests Facility (GPRTF) is assured by a MICATHERM S15 seal (part 10). A copper face gasket (part 14) provides the sealing between the casing and the nozzle.

The catalytic reactor is provided with five temperature taps realized by means of 1/16 NPT connectors welded on the outer wall of the thruster casing. The taps are spaced axially by 10 mm starting from the injection plate, and alternately staggered by ±60° with respect to the vertical meridional half-plane.

The thruster is mounted on a one degree-of-freedom dynamometric force balance (see Figure 3). In order to evaluate the performance of the thruster prototype and the catalytic reactor the following measurements are acquired:

- the chamber pressure, by means of a Kulite pressure transducer model XTM-190M-17 bar, which has been mounted recessed for protection from the high temperatures (part 18, Figure 1);
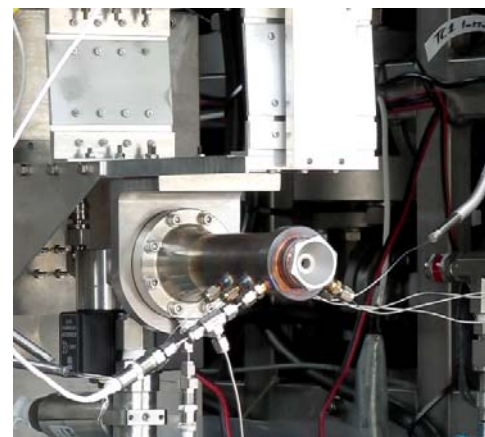

Figure 2. ALTA's GPRTF: thrust balance.

- the chamber temperature, by means of a 1 mm diameter K-type mineral-insulated thermocouple mounted on the combustion chamber housing by means of an adjustable 1/16'' NPT welded bushing, with the sensing tip located on the chamber axis;
- the pressure drop across the engine (injector + catalytic bed), by means of a FP2000 differential pressure transducer produced by Honeywell (500 psi range, 0.1% FSO accuracy), with the negative pressure tap in correspondence of the chamber pressure transducer (part 18) and the positive one placed upstream the hydrogen peroxide supply line connection to the thruster (part 12, Figure 1);
- the pressure after the injector, by means of a Kulite pressure transducer model XTM-190M-17 bar, which has been mounted recessed for protection from the high temperatures (part 17, Figure 1);
- the local catalyst temperature, by means of five 1 mm diameter K-type mineral-insulated thermocouples mounted on the catalytic bed housing with the sensing tips located on the bed axis;
- the thrust, by means of a subminiature compression load cell (Sensotec model 13) with 25 lbf FS and a maximum combined error (non-linearity, hysteresis and repeatability) of 0.9% FSO.
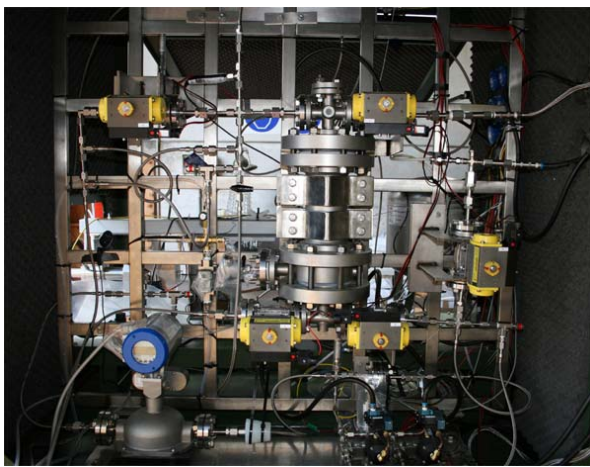

Figure 3. ALTA's GPRTF: feeding system.

The experimental campaign has been carried out in Alta's Green Propellant Rocket Test Facility (GPRTF, Figure 3), an easily reconfigurable and expandable experimental apparatus especially designed for performance characterization of small monopropellant (H_2O_2) and bipropellant (H_2O_2-hydrocarbon)[4,5,10,11,12] rocket engine prototypes and catalytic reactors operating at thrust levels in the 1-40 N and 25-100 N ranges. The facility mainly comprises the propellant feed systems and the thrust balance. All of the hydrogen peroxide lines and main tank are made of AISI 316 stainless steel internally coated with Teflon. Hydrogen peroxide is stored in a 2.5 liters tank and is pressurized by means of Nitrogen. Its physical conditions are continuously monitored by means of a J-type thermocouple and a gauge pressure transducer. If the peroxide starts to decompose, the tank can be vented to the atmosphere by means of a remotely controlled valve or, in the absence of the operator, by the combination of a relief valve and a burst disc calibrated for opening at suitably spaced pressure values. The hydrogen peroxide mass flow rate is controlled by means of interchangeable cavitating venturis and it is monitored by a Coriolis flowmeter. The operation of the venturi is continuously monitored by a differential and a downstream pressure transducer. The experiments reported in the present paper have been performed without the cavitating venturi.

Table 1. ALTA's GPRTF supply line sensors list.

Transducer	Model	Range	Accuracy	Location
Thermocouple J-type	6 mm OD, mineral-insulated, by Watlow	-40−750 °C	± 1.5 °C up to 375 °C	main tank
gauge pressure transducer	PTU60 model, by Swagelok	0−60 barg	± 0.43% FSO	main tank
differential pressure transducer	FP2000 model, by Honeywel	0−500 psid	± 0.1% FSO	across the venturi
gauge pressure transducer	PTU40 model, by Swagelok	0−40 barg	± 0.43% FSO	downstream of the venturi
Coriolis mass flow meter	MFS 7100 S04 model, by Krohne	0−100 kg/hr	± 0.1% measured value	downstream of the venturi

Table 1 reports the model, the physical range, the accuracy and the location of all the transducers installed in the GPRTF supply line.

A DC source, capable of supplying different output voltages, provides the transducers with the required electric excitations. The data coming from the sensors and transducers installed in the facility are acquired and transferred to a personal computer by means of a National Instruments acquisition board, capable of acquiring 32 analogic channels and 48 digital channels at a maximum sampling rate of 1.25 MS/sec. The acquisition board is connected to different SCXI conditioning and filtering modules, also produced by National Instruments. A LabVIEW® data acquisition and control program is used for real time display of the data and for recording all of the acquired signals. A 20 Samples/s acquisition rate has been selected for compatibility with the maximum speed of the acquisition board and of the personal computer CPU, which represents the most stringent speed limitation of the present experimental configuration. Pressure, mass flow rate and thrust signals have been low-pass filtered by means of a 10 Hz cut-off frequency analog Butterworth filter. A lower cut-off frequency (4 Hz) has been used for the temperature signals.
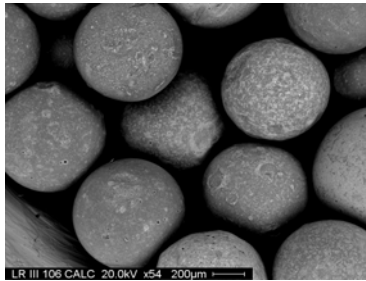
III. Catalyst

Figure 4. LR-III-106 catalyst sample.

A Pt/$\alpha-$Al$_2$O$_3$ catalyst, named LR-III-106, has been selected for the experimental campaign reported in the present paper. It has been prepared using 0.6 mm spheres of $\alpha-$Al$_2$O$_3$ with a BET surface area of 4 m^2/g produced by SASOL GmbH. The catalyst has been prepared using a proprietary coating technique developed by Alta S.p.A. in collaboration with the Department of Chemistry and Industrial Chemistry of Pisa University, Italy. Endurance tests on LR-III-106 catalyst had been already performed with the same thruster prototype at a lower mass flux ($G\approx$12 kg/(m^{2}s), Pasini et al.[5]): the bed was able to decompose up to 13 kg of 90% hydrogen peroxide, equivalent to 2500 s of thruster continuous operation, exhibiting C-Star efficiency higher than 95%. Figure 4 shows a scanning electron micrograph of the LR-III-106 (54×) catalyst, while Table 2 summarizes its main characteristics.

A single 30 cm^3 catalytic bed has been used for the experimentation hereafter reported.

Table 2. Main characteristics of LR-III-106 catalytic system.

Identification code	Catalyst	Support	Nominal metal load (wt %)	SEM metal load (wt%)
LR-III-106	Pt/$\alpha-$Al$_2$O$_3$	0.6/4	1	3

IV. Experimental Results and Discussion

A. Performance Parameters for H$_2$O$_2$ Catalytic Beds

The typical parameters used for assessing the effectiveness of catalytic beds in decomposing HP for thrust generation are the temperature efficiency ($\eta_{\Delta T}$) and the characteristic velocity efficiency (η_{c*}).

The temperature efficiency is defined as:

$$\eta_{\Delta T} = \frac{T_c - T_{amb}}{T_{ad} - T_{amb}} \tag{1}$$

and it expresses how close the measured chamber temperature is to the adiabatic temperature corresponding to complete decomposition of the propellant.

On the contrary, the $c*$ efficiency expresses the ratio between the measured characteristic velocity and the theoretical one, computed using the 1D ideal rocket equations and the nominal adiabatic decomposition temperature (T_{ad}) of the propellant, as reported in the following equation:

$$\eta_{c*} = \frac{c^*_{exp}}{c^*_{theo}} = \frac{\dfrac{p_c A_t}{m}}{\sqrt{\dfrac{RT_{ad}}{\gamma}}\left(\dfrac{\gamma+1}{2}\right)^{\frac{\gamma+1}{2(\gamma-1)}}} \tag{2}$$

While the temperature efficiency mainly expresses the effectiveness of the catalytic reactor, which can be not necessarily followed by a thrust chamber, the *c** efficiency is the key propulsive parameter that takes into account both the chemical performance of the catalyst, which can reduce the decomposition temperature below its nominal value, and the non-idealities of the gas transit through the thrust chamber and the convergent part of the expansion nozzle.

In propulsive applications, also the pressure drop across the catalytic bed is an important operational parameter because it affects the magnitude of the feed pressure and consequently the weight of the propellant storage system.

Finally, in rocket engines for RCS, the transient start-up is crucial in order to satisfy the requirements of the attitude control system. In general, the time-evolution of a thrust profile can be separated into different sections: ignition delay, thrust rise time and thrust decay time[13]. The ignition delay, called decomposition delay in monopropellant rockets, consists in the time required for the thrust to reach 1% of its nominal value since the opening of the firing valve. The thrust rise time refers to the time elapsed between 1% of the nominal value to 90%. The decay time concerns with the final transient of the thrust and it is the time between the shutoff of the valve and the reaching of 10% of the steady-state value of the thrust.

Since the behavior of the thrust in the rocket can be approximated as a first order system with respect to an impulsive variation of the mass flow rate, the typical time constant of first order system (defined as the time needed after the ignition delay to reach $(1-e^{-1})$ of the nominal value) has been evaluated and reported in the next section.

B. Tests on LR-III-106 at G=55 kg/(m²s)

The experimental campaign on the LR-III-106 catalyst has consisted of five firings with the following duty cycle: a 46 s cold-start firing, followed by three 10 s pulses separated by 10 s pauses and a final hot-start firing, as shown respectively in Figure 5, Figure 6 and Figure 7. In all the firings, the steady state value of the thrust was 32 N and the chamber pressure reached values up to 22.5 bar. Especially in the first cold-start firing, the mass flow rate profile has been characterized by a strong overshoot peak caused by the absence of the cavitating venturi. Contrary, this peak almost disappeared in the last two firings, when the temperature of the catalytic bed was high enough to vaporize the propellant and, consequently, rapidly pressurize the thrust chamber.

An anomalous peak in the pressure measured at the inlet of the catalytic bed has been detected in the first three firings, as reported in Figure 5 and Figure 6. The magnitude of this overpressure has been quite high; the most unexpected aspect is that the profiles of the chamber pressure, the thrust and the mass flow rate are completely not affected by this phenomenon. A possible explanation for this anomaly can be found in the topology of the pressure tap. Figure 1 reports a cross section of the monopropellant prototype that shows the location of the pressure tap before the inlet of the catalytic bed. This pressure transducer has been mounted recessed and, therefore, there is some empty volume in front of it. Probably, at the beginning of the firing this small empty volume has been filled by liquid hydrogen peroxide. During the firing, the thermally conducted energy through the metal casing of the prototype has allowed for the thermal decomposition of this small amount of hydrogen peroxide and a consequent pressure increase in the small chamber in front of the pressure transducer due to the choking of the narrow connecting tube. This justifies both the strong overpressure locally measured by the transducer and the almost negligible influence on the chamber pressure, the thrust and the mass flow rate due to the paltry amount of propellant involved.
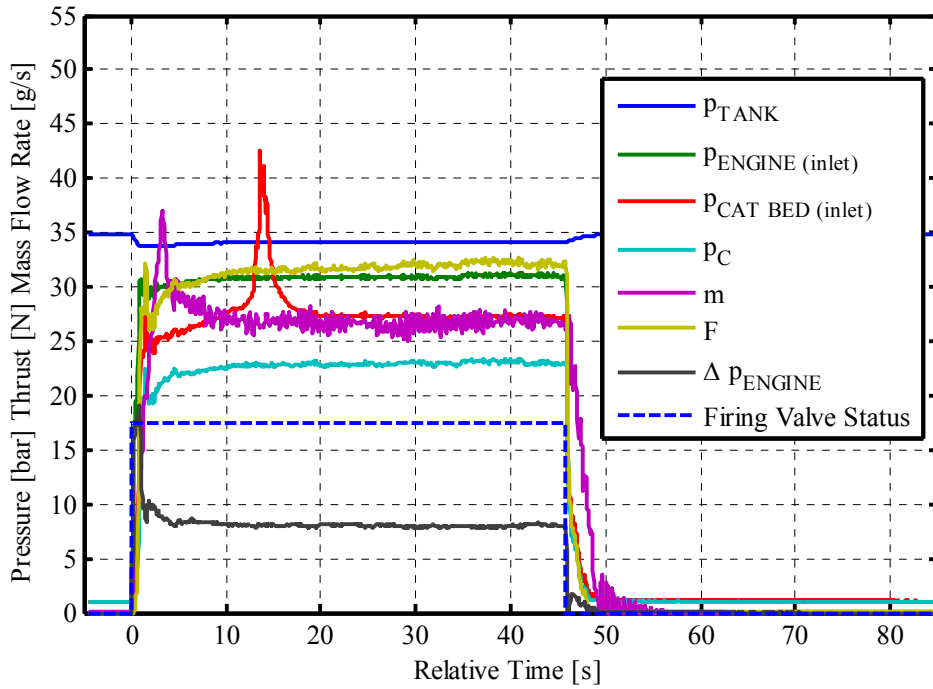
Figure 5. Initial cold-start firing: pressure, mass flow rate and thrust profiles as functions of the Relative Time.
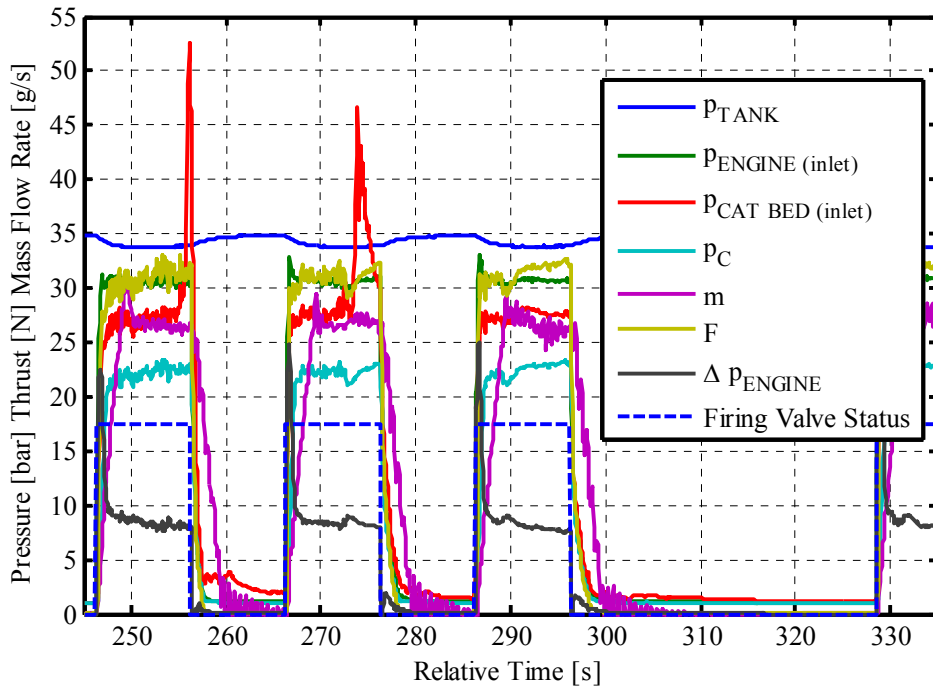

Figure 6. Intermediate three pulses: pressure, mass flow rate and thrust profiles as functions of the Relative Time.
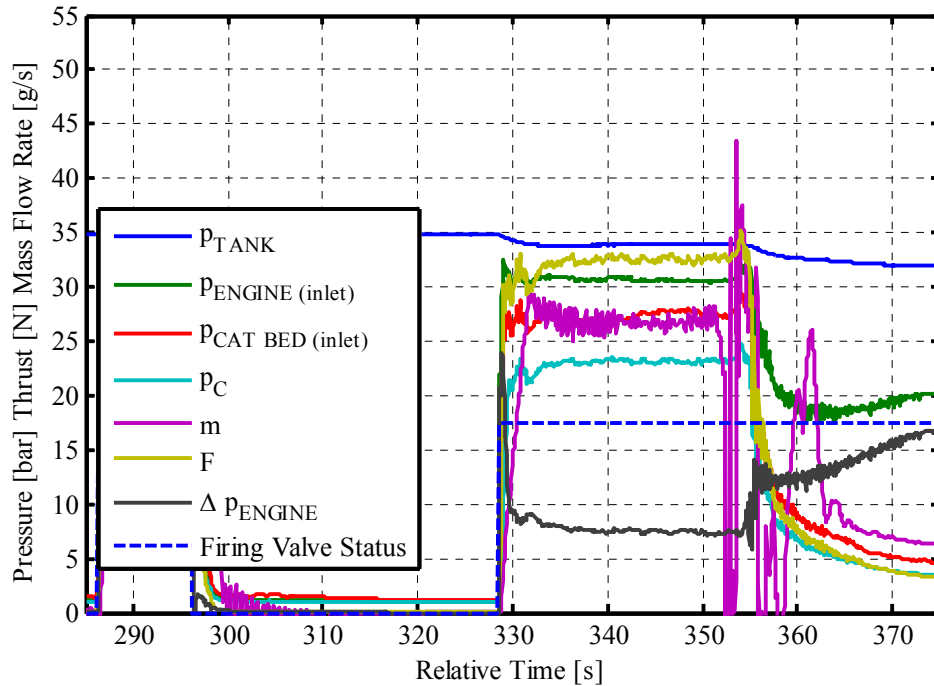
Figure 7. Final hot-start firing: pressure, mass flow rate and thrust profiles as functions of the Relative Time.

Figure 8 reports the time-evolution of the temperatures inside the catalytic reactor as functions of the cumulative time from the beginning of the test. In particular, the experimental data have been plotted only when the firing valve was open and, consequently, the dead times between two firings are not reported.

Despite the high value of the mass flux only the first thermocouple, located at 15 mm from the inlet of the bed, has been affected by intermittent flooding. Sometimes, in fact, this thermocouple has measured a temperature next to the vaporization temperature of the reacting mixture detecting the presence of a multiphase flow in this region of the reaction chamber.

The temperature profiles along the catalytic bed have not been particularly smooth and the mean values registered by all the temperature sensors, except for the first thermocouple, are about 700 °C. Therefore, the catalytic bed is oversized for these operational parameters and, probably, half of its length would be enough to obtain the same propulsive performance.
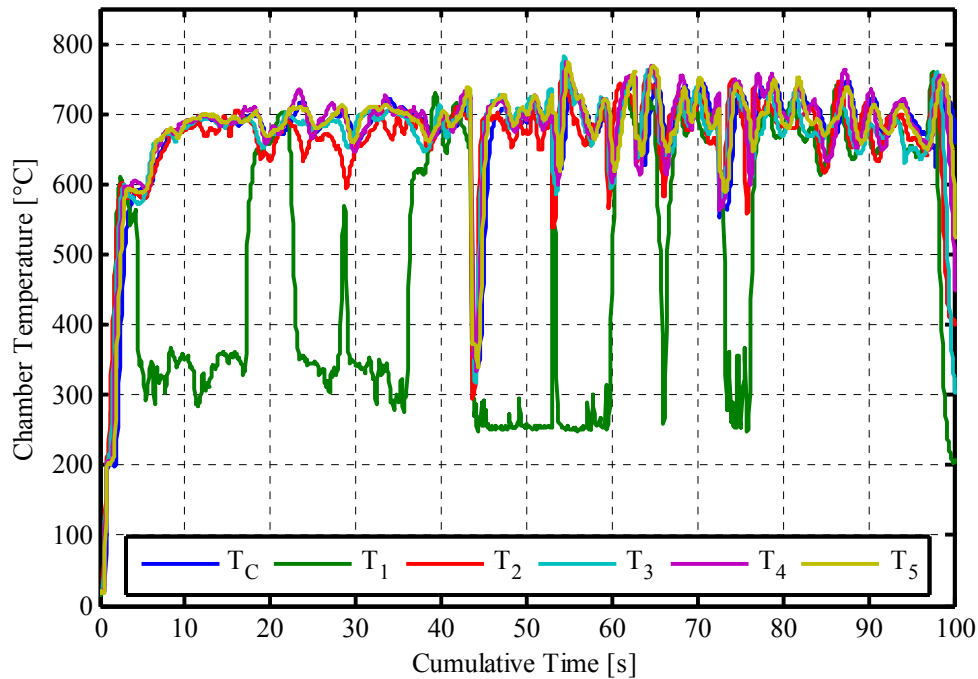
91.1% H_2O_2 LR-III-106

Figure 8. Temperature profiles inside the catalytic bed as functions of the Cumulative Time.

Figure 8 shows the time-evolution of the pressures along the catalytic reactor as functions of the cumulative time from the beginning of the test. In general, pressure profiles have been smooth except for the anomalous peaks already explained as a local phenomenon inside the pressure tap of the absolute transducer at the inlet of the bed. While the signal of the differential pressure transducer, used for measuring the pressure losses across the injector and the catalytic bed, has been constant, the profiles of the pressure drop across the injector and the bed have been affected by the local phenomenon because they have been computed using the output of the transducer located at the inlet of the bed.

In steady state conditions, the feed pressure of the engine has been 30.5 bar and the pressure losses have been respectively 4 bar across the injector and 4 bar across the catalytic bed yielding to a chamber pressure equal to 22.5 bar.
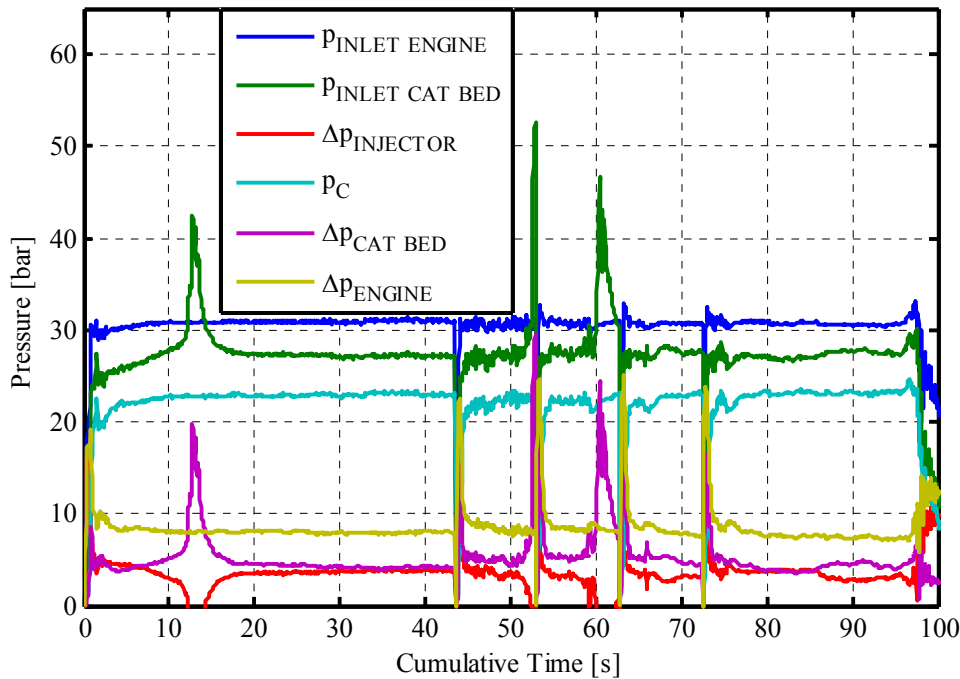
Space Propulsion 2010, 3-6 May 2010, San Sebastian, Spain

91.1% H_2O_2 LR-III-106

Figure 9. Pressure profiles inside the prototype as functions of the Cumulative Time.

The propulsive performance has been summarized in Figure 10 by plotting the $c*$ and temperature efficiencies as a function of the cumulative time. In particular, the characteristic velocity efficiency has been higher than 95% while the temperature efficiency has overcome the threshold of the 90%.

The time-evolution of the efficiencies has shown no degradation of the performance but a slight improvement due to the heating of the prototype that has reduced the heat losses of the decomposing flow.

In order to investigate the effects of the catalytic bed temperature on the transient start-up, the first 5 seconds of a cold-start (first) and an hot-start (fourth) firing are reported in Figure 11.

For a better understanding of the experimental data, it is worth noticing that in all the reported tests the time constant of the flowmeter has been set to 3 seconds while the natural frequency of the pressure transducer is 425 kHz. After the opening of the valve, the physical variation of the mass flow rate is almost impulsive, while the time response of the flowmeter output reaches the steady-state value after some seconds due to the high value of the time constant. Contrary, the output profile of the pressure transducer is due to the first-order behavior of the thrust chamber with respect to an impulsive variation of the mass flow rate and not to the response time of the sensor which is much higher.

According to the previous remarks, it is possible to associate the overshot of the pressure transducer to the peak of the mass flow rate even if they have been recorded at different values of the Cumulative Time because of the different time constants of the sensors. The set-up of the facility has been characterized by the absence of the cavitating venturi, which had been used in all the previous experiments at Alta. In this configuration, the mass flow rate is proportional to the pressure drop across the injector and, therefore, is affected by the pressure inside the thrust chamber. As previously explained, the overshot peak of mass flow rate has been measured in the cold-start (left part of Figure 11) while it has almost disappeared in the hot firing (right part of the same figure).

Table 3 reports the analysis of the thrust profile transients of the different firings in terms of decomposition delay, rise time, decay time and time constant. In particular, the comparison between the first and the fourth firings suggests that both the decomposition delay and the thrust rise time have been strongly affected by the initial temperature while, obviously, the decay time has been mainly influenced by the final temperature. The 400 ms decomposition delay of the cold-start has been reduced to 180 ms in the hot-start, while the thrust rise time has been decreased from 994 ms to 230 ms. The thrust decay time has been almost the same (~1400 ms) in both the experiments.
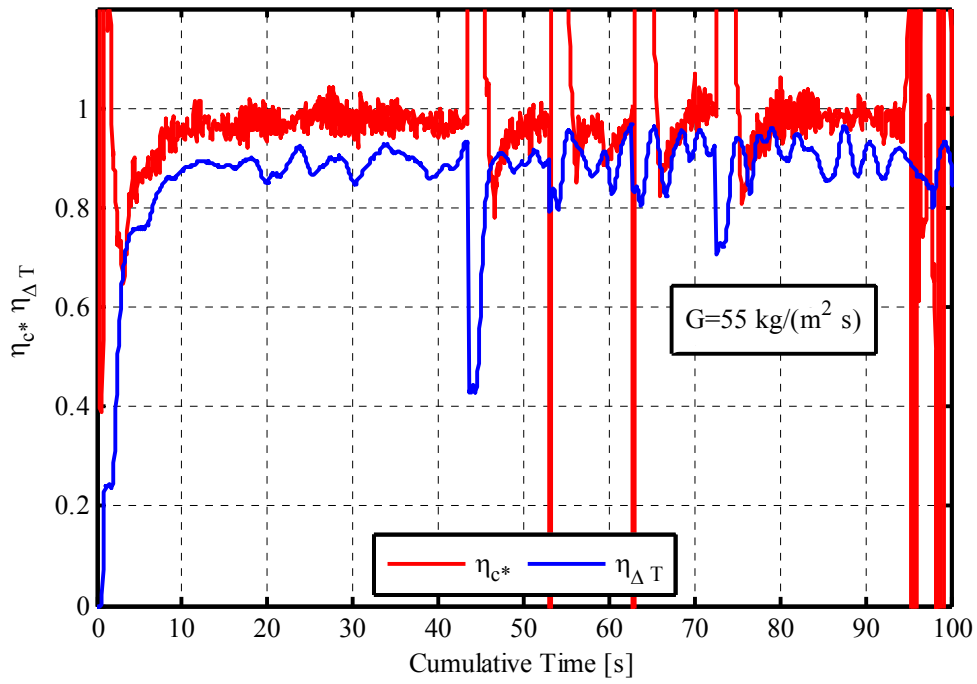
91.1% H_2O_2 LR-III-106

Figure 10. Comparison between *c** and temperature efficiencies at *G*=55 kg/(m²s) as functions of the Cumulative Time.

Table 3. Response time.

Mass Flux [kg/(m²s)]	Firing Number	Initial Temperature [°C]	Decomposition Delay [ms]	Thrust Rise Time [ms]	Thrust Decay Time [ms]	Time Constant [ms]
55	I	20	400	994	1460	495
	II	350	210	1040	930	280
	III	620	150	320	1240	210
	IV	630	180	230	1400	130
12	I	20	470	16000	6200	9000
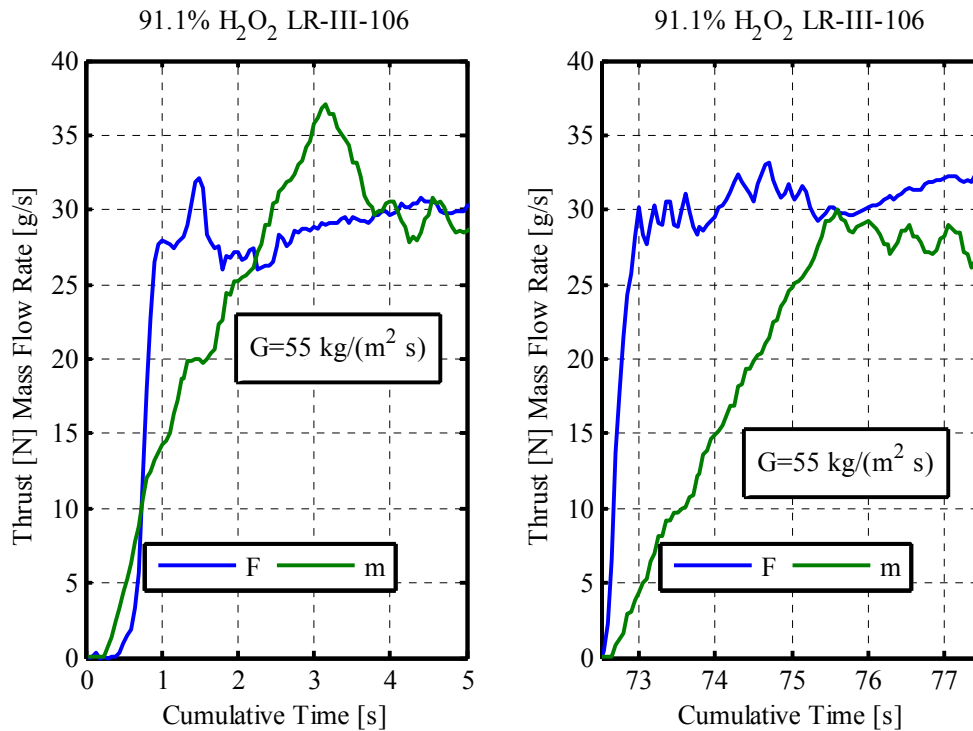
Figure 11. Transient start-up: comparison between cold (left) and hot (right) firings.

C. Influence of the Mass Flux on the Transient Start-Up

The results of the endurance tests on LR-III-106 catalyst (Pasini et al.[5]), performed with the same catalytic bed at lower mass flux ($G \approx 12$ kg/(m²s)) and pressure ($p_c \approx 17$ bar), have been used to investigate the influence of the operational parameters on the transient start-up.

The initial time-evolutions of the chamber pressure and the mass flow rate for two cold-start firings performed with fresh catalyst at different mass fluxes are reported in Figure 12. In both the experiments, the almost impulsive variation of the mass flow rate is detected by the flowmeter through the typical response to a step for a system with a time constant equal to 3 seconds. In the experiment at $G \approx 12$ kg/(m²s), the presence of the cavitating venturi is evident in the absence of the strong overshot peak (Figure 12, left) detected in the test without flow controller devices in the profiles of both pressure and mass flow rate (Figure 12, right).

While the decomposition delay has been almost the same in both the tests, as reported in Table 3, the thrust rise has been strongly affected by the mass flux. In fact, an increase of almost five times has implied a reduction of the rise time of more than one order of magnitude: from 16000 ms to 994 ms. Contrary, the variation of the thrust decay time has been of the same magnitude of the variation of the mass flux.

Figure 13 and Figure 14, respectively, report the temperature profile inside the catalytic bed at low and high mass flux. In tune with the previous results on the thrust, the transient phase in the temperature profiles has been reduced at the higher mass flux. In particular, the time required for the vaporization detected by the thermocouple inside the chamber has been decreased from 10 s to 2 s, following the same ratio of the mass flux values.

Furthermore, it is worth noticing the partially decomposed flow detected by the first thermocouple in the experiment at high mass flux due to the reduction of the residence time in the decomposition process.

Finally, in order to investigate the influence of the mass flux on the propulsive performance, the $c*$ and the temperature efficiencies at lower mass flux are reported in Figure 15 as functions of the first 100 seconds of Cumulative Time. Despite the different values of bed load, the steady-state value of the characteristic velocity efficiency has been the same, even if its profile at lower mass flux has been much smoother. On the other hand, the temperature efficiency has been higher at lower mass flow rate.
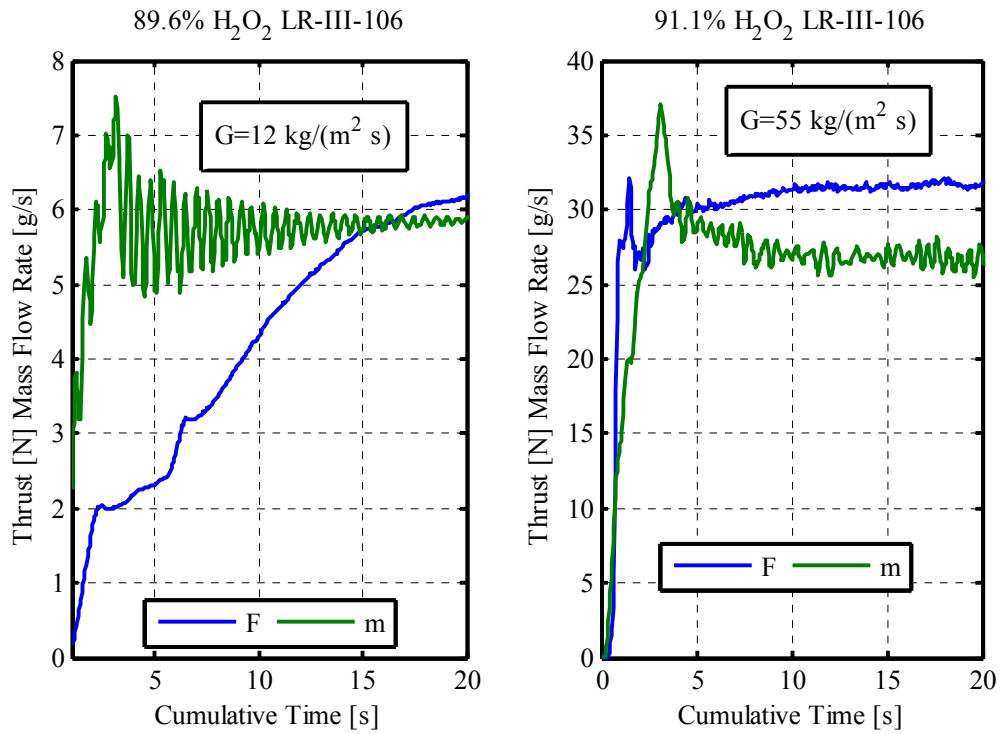
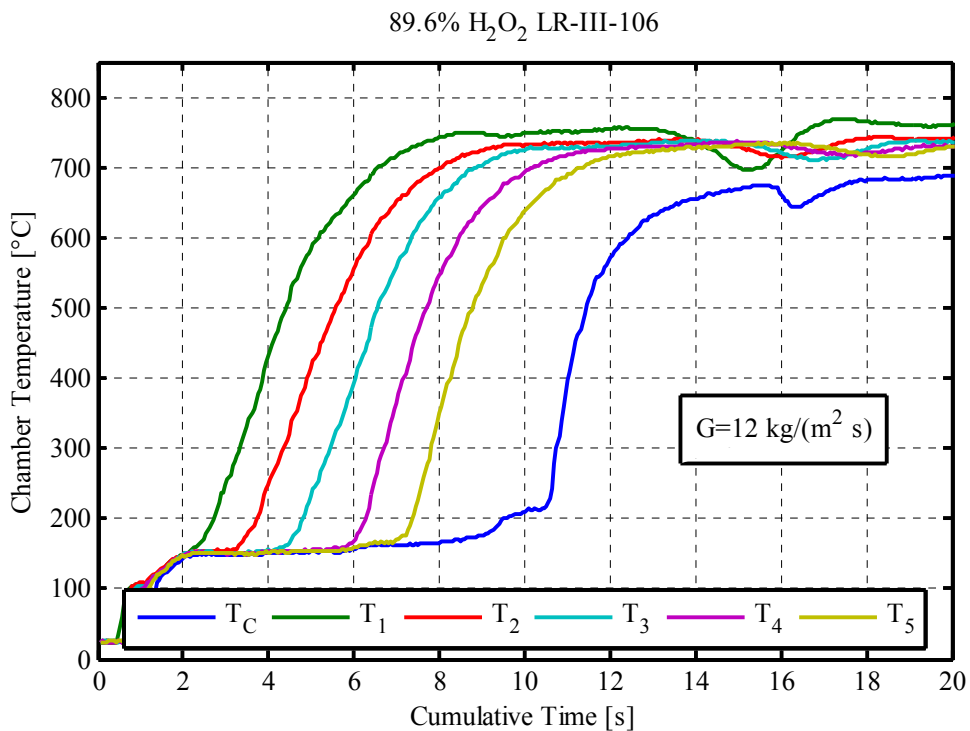**Figure 12. Transient start-up: comparison between different values of the mass flux.**

Figure 13. Temperature profiles inside the catalytic bed for a cold-start at *G*=12 kg/(m²s)

In general, the chamber temperature, T_c, is a function of the fraction of the decomposed mass flow rate. In particular, the decomposed molar flow rate can be obtained by integrating the volumetric reaction rate on the catalytic bed volume. In an ideal case the temperature of the reaction products at the exit of the bed can be associated, through an enthalpic balance, to the total decomposed moles per unit time. Extrapolating this quantity from experimental data, it appears to increase almost linearly with time.

Assuming, as a first approximation, that the decomposition capability of the bed is linear with its mean temperature,

$$\int_{V_{bed}} \dot{r} \, dV \propto \bar{T}_{bed} \tag{3}$$

the time derivative of the temperature of the bed, evaluated assuming a convective heat transfer between the reacting flow and the pellets of the catalytic bed,

$$\frac{\partial \bar{T}_{bed}}{\partial t} = \frac{S_{bed}}{m_{bed}} \frac{c_{p \, flow}}{c_{p \, bed}} \left(\frac{1}{\varepsilon_{bed}} \right)^{2/3} G C_h \Delta \bar{T} \tag{4}$$

can be used to calculate the time derivative of the decomposition capability:

$$\frac{\partial \int_{V_{bed}} \dot{r} \, dV}{\partial t} \propto \frac{S_{bed}}{m_{bed}} \frac{c_{p \, flow}}{c_{p \, bed}} \left(\frac{1}{\varepsilon_{bed}} \right)^{2/3} G \tag{5}$$

In the experiments presented in this paper, all the parameters related to the catalytic bed are constant except for the mass flux and, consequently, the time derivative of the decomposition capability should be proportional to G. In order to verify the previous analysis, the time elapsed between two different degrees of decomposition (T_c) has been compared to the mass flux of the experiment. In particular, the time necessary for reaching the dry-out condition has been respectively 10 s and 2 s at low and high mass flux and, consequently, the ratio of these times is almost equal to the ratio of G. This correlation is also verified for the experimental points referring to 100°C and 500°C. In this case, the time necessary to pass from the lower temperature to the higher one is, respectively, 10.07 s and 2.18 s for low and high bed load.
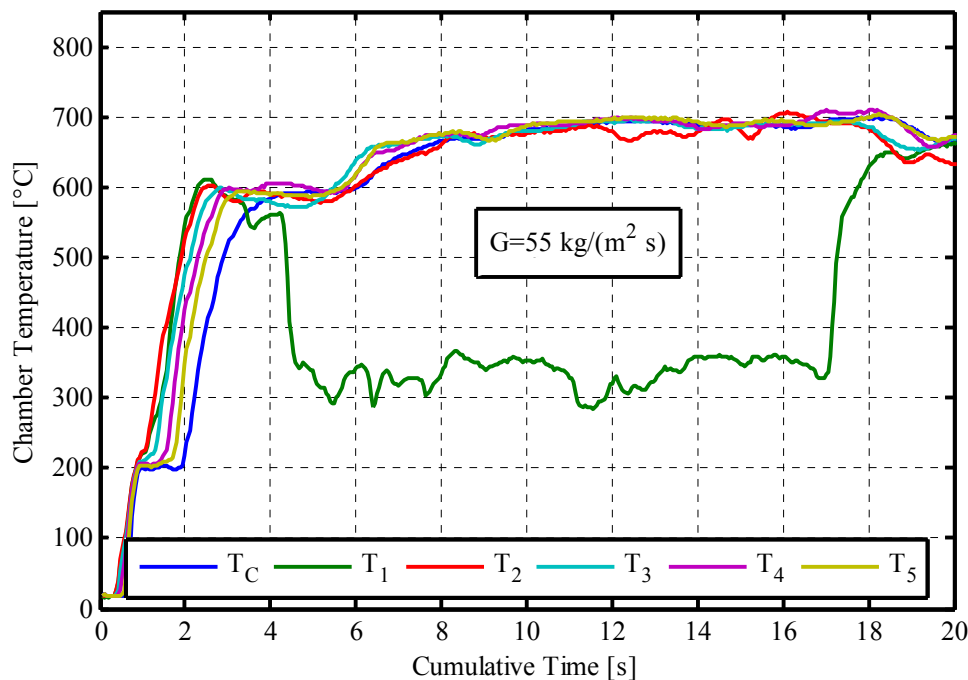

Figure 14. Temperature profiles inside the catalytic bed for a cold-start at G=55 kg/(m^{2}s)

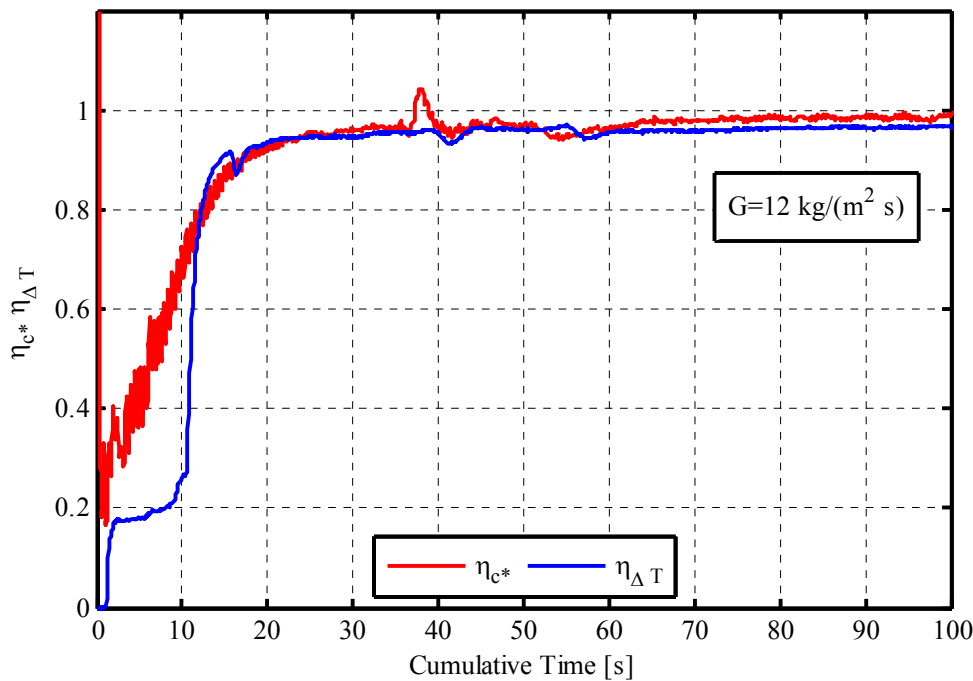**Figure 15. Comparison between *c** and temperature efficiencies at *G*=12 kg/(m²s) as functions of the Cumulative Time.**

V. Conclusions

The LR-III-106 catalyst arranged in a 30 cm³ catalytic bed, already successfully tested at lower mass flux[5], has shown excellent decomposition properties at $G = 55$ kg/(m²s) too. Its high characteristic velocity efficiency ($\eta_{c*} >$ 95%) has remained unchanged in both the configurations and the information regarding the temperature inside the catalytic bed suggests that, even for the higher mass flux, the length of the bed is oversized. Furthermore, the very good results of the endurance test at lower mass flux look promising for a future endurance test at higher bed load.

The time response of the prototype has been strongly reduced by increasing the mass flux. In particular, the thrust rise time of the cold-start firing has been decreased more than one order of magnitude and future improvements can be achieved also considering that the prototype used in the experiment is not optimized for the reduction of the empty volumes inside the thruster.

The analysis of the initial transient of cold and hot-start firings has indicated that both the decomposition delay and the thrust rise time are influenced by the temperature, while, for cold-start tests, the variation of the mass flux does not strongly affect the decomposition delay.

Finally, the presence of local overpressures measured by the pressure transducer located before the inlet of the bed, due to the thermal decomposition of the hydrogen peroxide trapped in the pressure tap, suggests the suitability of a configuration of the pressure tap that avoids the possibility of trapping liquid hydrogen peroxide.

References

[1]Romeo L., Torre L., Pasini A., Cervone A., d'Agostino L., Calderazzo F., *"Performance of Different Catalysts Supported on Alumina Spheres for Hydrogen Peroxide Decomposition",* AIAA Paper 2007-5466, 43rd AIAA/ASME/SAE/ASEE Joint Propulsion Conference, Cincinnati, Ohio, USA, July 2007.

[2]Romeo L., Torre L., Pasini A., d'Agostino L., Calderazzo F., *"Development and Testing of Pt/Al$_2$O$_3$ Catalysts for Hydrogen Peroxide Decomposition",* 5th International Spacecraft Propulsion Conference and 2nd International Symposium on Propulsion for Space Transportation, Heraklion, Crete, Greece, 5-8 May 2008.

[3]Romeo L., Genovese C., Torre L., Pasini A., Cervone A., d'Agostino L., Centi G., Perathoner S*., ''Use of Pt/Ce$_x$O$_2$-Zr$_{1-x}$O$_2$/Al$_2$O$_3$ as Advanced Catalyst for Hydrogen Peroxide Thrusters'',* AIAA Paper 2009-5637 45th AIAA/ASME/SAE/ASEE Joint Propulsion Conference, Denver, Colorado, USA, August 2009.

[4]Pasini A., Torre L., Romeo L., d'Agostino L., Cervone A., Musker A., *"Experimental Characterization of a 5N Hydrogen Peroxide Monopropellant Thruster Prototype",* AIAA Paper 2007-5464, 43rd AIAA/ASME/SAE/ASEE Joint Propulsion Conference, Cincinnati, Ohio, USA, July 2007.

[5]Pasini A., Torre L., Romeo L., Cervone A., d'Agostino L., *''Endurance Tests on Different Catalytic Beds for H$_2$O$_2$ Monopropellant Thrusters''* AIAA Paper 2009-5638 45th AIAA/ASME/SAE/ASEE Joint Propulsion Conference, Denver, Colorado, USA, August 2009.

[6]Ventura M., Wernimont E., *"Advancements in High Concentration Hydrogen Peroxide Catalyst Beds,"* AIAA Paper 2001-3250, AIAA/ASME/SAE/ASEE Joint Propulsion Conference and Exhibit, July 2001.

[7]Wernimont, E. Durant D., , *"State of the Art High Performance Hydrogen Peroxide Catalyst Beds,"* AIAA Paper 2004-4147, AIAA/ASME/SAE/ASEE Joint Propulsion Conference and Exhibit, July 2004.

[8]Scharlemann C., Schiebl M., Marhold K., Tajmar M., Miotti P., Kappenstein C., Batonneau Y., Brahmi R., Hunter C, *"Development and Test of a Miniature Hydrogen Peroxide Monopropellant Thruster"*, AIAA-06-4550, 42nd AIAA/ASME/SAE/ASEE Joint Propulsion Conference & Exhibit, July 9-12, 2006, Sacramento, California .

[9]Sungyong A., Kwon S., *"Catalyst Bed Sizing of 50 Newton Hydrogen Peroxide Monopropellant Thruster"* AIAA Paper 2008-5109, 44th AIAA/ASME/SAE/ASEE Joint Propulsion Conference and Exhibit, July 2008.

[10]Pasini A., Torre L., Romeo L., Cervone A., d'Agostino L., *"Testing and Characterization of a Hydrogen Peroxide Monopropellant Thruster"*, Journal of Propulsion and Power, Vol.24, N°3, May-June 2008.

[11]Torre L., Pasini A., Romeo L., d'Agostino L., *"Firing Performances of Advanced Hydrogen Peroxide Catalytic Beds in a Monopropellant Thruster Prototype"* AIAA Paper 2008-5575, 44th AIAA/ASME/SAE/ASEE Joint Propulsion Conference & Exhibit, July 20-23, 2008, Hartford, Connecticut, USA.

[12]Torre L., Pasini A., Romeo L., Cervone A., d'Agostino L., *"Performance of a Monopropellant Thruster Prototype Using Advanced Hydrogen Peroxide Catalytic Beds"*, Journal of Propulsion and Power, Vol.25, N°6, November-December 2009.

[13]Brown C. D., *"Elements of Spacecraft Design"*, AIAA, Reston, VA, 2002.